frontiers | Frontiers in Nuclear Engineering

TYPE Original Research
PUBLISHED 28 February 2024
DOI 10.3389/fnuen.2024.1347322



OPEN ACCESS

EDITED BY
Anne Campbell,
Oak Ridge National Laboratory (DOE),
United States

REVIEWED BY
Charles M. Folden,
Texas A and M University, United States
Tashiema Ulrich,
Oak Ridge National Laboratory (DOE),
United States

*CORRESPONDENCE
Jessica Blenkinsop,
Jessica.blenkinsop@uknnl.com

RECEIVED 30 November 2023
ACCEPTED 16 February 2024
PUBLISHED 28 February 2024

CITATION
Blenkinsop J, Rivonkar A, Robin M, Carey T, Dunnett B, Suzuki-Muresan T, Percin C, Abdelouas A and Street J (2024), Methods for the destruction of oxalic acid decontamination effluents.
*Front. Nucl. Eng.* 3:1347322.
doi: 10.3389/fnuen.2024.1347322



# Methods for the destruction of oxalic acid decontamination effluents

Jessica Blenkinsop[1]*, Aditya Rivonkar[2], Mathurin Robin[2], Thomas Carey[1], Barbara Dunnett[1], Tomo Suzuki-Muresan[2], Cavit Percin[2], Abdesselam Abdelouas[2] and Jonathan Street[3]

[1]National Nuclear Laboratory (NNL), Cumbria, United Kingdom, [2]Subatech Laboratory, IMT Atlantique CNRS/N2P3 Nantes University, Nantes, France, [3]Sellafield Ltd., Cumbria, United Kingdom

Oxalic acid is encountered within industrial processes, spanning from the nuclear sector to various chemical applications. The persistence and potential environmental risks associated with this compound underscore the need for effective management strategies. This article presents an overview of different approaches for the destruction of oxalic acid. The study explores an array of degradation methodologies and delves into the mechanistic insights of these techniques. Significant attention is channeled towards the nuclear industry, wherein oxalic acid arises as a byproduct of decontamination and waste management activities. An integral aspect of decommissioning efforts involves addressing this secondary waste-form of oxalic acid. This becomes imperative due to the potential release of oxalic acid into waste streams, where its accommodation is problematic, and its capacity to solubilize and transport heavy metals like Pu is a concern. To address this, a two-tiered classification is introduced: high concentration and low concentration scenarios. The study investigates various parameters, including the addition of nitric acid or hydrogen peroxide, in the presence of metallic ions, notably $Mn^{2+}$ and $Fe^{2+}$. These metallic ions are common components of effluents from metallic waste treatment. Additionally, the impact of UV light on degradation is explored. Investigations reveal that at high concentrations and with the influence of hydrogen peroxide, the presence of metallic cations accelerates the rate of destruction, demonstrating a direct correlation. This acceleration is further enhanced by exposure to UV light. At low concentrations, similar effects of metallic cations are observed upon heating the solution to 80°C. The rate of destruction increases proportionally with hydrogen peroxide concentration, with an optimal oxalic acid to hydrogen peroxide ratio of 1:100. Interestingly, a low-power UV light exerted no discernible effects on the destruction rate; heating alone proved sufficient. In essence, regardless of concentration, the degradation of oxalic acid with hydrogen peroxide experiences acceleration in the presence of metallic ions such as $Mn^{2+}$ and $Fe^{2+}$.

KEYWORDS

**oxalic acid, destruction, nitric acid, UV light, hydrogen peroxide, nuclear decommissioning**

# 1 Introduction

Oxalic acid ($C_2H_2O_4$) is a naturally-occurring organic compound found in plants (Mitchell et al., 2019). The use of oxalic acid is observed over a variety of industries and applications. This ranges from the removal of rusts for managing the environmental quality of metals (Wang Q et al., 2023), the conservation of contemporary acrylic paintings (Solbes-García et al., 2017) and the synthesis of graphitic carbon nitrides (Zhang et al., 2022), among many others.

Decontamination is an essential step in the life cycle of nuclear power plants to limit the potential release of radioactive species and reduce the risk to those working on plants. Contamination may be deemed "fixed", where it is firmly adhered to a surface, or "loose", where it may be easily removed from a surface via non-destructive methods; both of these present individual challenges. While washes with water or weakly concentrated nitric acid may be suitable for loose contamination, more invasive techniques may be required for the removal of fixed contamination of metal surfaces. Some decontamination methods explored include, but are not limited to the implementation of laser technology (Wang F et al., 2023), plasma decontamination (Zhong et al., 2021) as well as chemical decontamination encompassing the use of gels and foams (Gossard et al., 2022) and reagents like oxalic acid (Zhong et al., 2021).

Oxalic acid is known to strongly solubilize most iron oxides (Ocken, 1999). It is used as a rust-removal complexing agent that is also good for decontaminating highly damaged corroded surfaces. Oxalic acid dissolves deposited $MnO_2$. It can also serve as a corrosion inhibitor for carbon steels, limiting over-aggressive digestion during decontamination and so protecting the structural integrity of structures made of such steel. When oxalic acid is used in concentrations of less than 1 wt%, the decontamination process can be slow but has minimal impact on the corrosion of the metal surfaces. Whereas at higher concentrations, typically up to 10 wt%, the decontamination coefficient and treatment time are optimized, but corrosion increases along with chemical secondary waste requiring treatment (Zhong et al., 2021). The treatment of this oxalic acid rich secondary effluents is also an important part of decommissioning activity; this is a necessity due to the potential release of oxalic acid into waste streams where it is unable to be accommodated, or the ability of oxalic acid to solubilize and carry heavy metals such as Pu into waste streams, increasing the criticality risk (Orr et al., 2015).

Oxalic acid can be harmful to both humans and the environment when not properly handled or disposed of. High concentrations of oxalic acid can cause skin and eye irritation, respiratory problems, and even kidney failure (Kliegman and Geme, 2019). Therefore, it is essential to understand the methods for the destruction of oxalic acid to minimize its impact on the environment and human health. Methods for the destruction of oxalic acid to eliminate the risks associated with the secondary waste have been identified in literature. Some techniques, which may be particularly challenging to deploy on licensed nuclear sites and were therefore discarded, include electrolysis (Martinez-Huitle et al., 2004; Shih et al., 2019), ultrasonic degradation (Dükkanci and Gündüz, 2006) and catalytic wet air oxidation (Lee and Kim, 2000; Santos et al., 2021). Other methods from literature which were assessed to be more compatible with nuclear plant operations due to their ease of implementation, potentially using existing plant infrastructure, were identified to be heating with nitric acid (Mason et al., 2008) alongside manganous nitrate ($Mn(NO_3)_2$) (Kubota, 1982; Nash, 2012) and hydrogen peroxide ($H_2O_2$) (Berry, 1957; Chung et al., 1995; Kim et al., 2000), and well as ultra-violet (UV) light (Beltrán et al., 2002) and ozonation (Ketusky and Subramanian, 2012; Martino et al., 2012). These techniques–thought to be more appropriate for use on nuclear power plants–have been experimented with, as outlined in this paper.

Hydrogen peroxide is used because of the safety of the manipulation and the low cost of the reagents. In the presence of hydrogen peroxide, oxalic acid decomposes to form water and carbon dioxide as shown in Equation 1. UV acts as a catalyst in this reaction and speeds up the process. In parallel, hydrogen peroxide decomposes by a disproportionation reaction to generate water and oxygen, seen in Eq. 2 (Kim et al., 2000).

$$H_2O_2 + H_2C_2O_4 \rightarrow 2CO_2 + 2H_2O \quad (1)$$

$$H_2O_2 \rightarrow H_2O + \frac{1}{2}O_2 \quad (2)$$

In addition to hydrogen peroxide used during the process, it is possible to use manganese as a cation or manganese oxide to increase the reaction kinetics. Indeed, in the presence of nitric acid, manganese is a very powerful catalyst for oxidizing organic compounds such as oxalic acid (Saeed et al., 2013), even in low concentration (few mM). In the case of the Chemical Oxidation Reduction Decontamination (CORD) process, discussed later, various metals are present in solution, including manganese. That is why the catalytic reaction is studied here.

The presence of iron also plays a significant role during this process, acting as the Fenton reagent. Hydrogen peroxide oxidizes iron (II) to iron (III) and produces a hydroxyl radical and a hydroxide ion via the Fenton reaction mechanism shown in Eqs 3–5 (Metelitsa, 1971; Pawar and Gawande, 2015; Haber et al., 1934; Brillas et al., 2009). Iron (III) is then reduced back to iron (II) by another molecule of hydrogen peroxide, producing a hydroperoxyl radical and a proton as seen in Eq. 4. This results in the disproportionation of hydrogen peroxide to create two different oxygen-radical species, with water ($H^+ + OH^-$) as a byproduct.

$$Fe^{2+} + H_2O_2 + H^+ \rightarrow Fe^{3+} + OH^{\cdot} + H_2O \quad (3)$$

$$Fe^{3+} + H_2O_2 \rightarrow Fe^{2+} + HO_2^{\cdot} + H^+ \quad (4)$$

$$RH + OH^{\cdot} \rightarrow R^{\cdot} + H_2O \quad (5)$$

The free radicals generated by this process then engage in secondary reactions. The hydroxyl radical is a powerful, non-selective oxidant. Fenton's reagent is a rapid and exothermic method of oxidizing organic compounds. It results in the oxidation of contaminants to primarily carbon dioxide and water (Kim et al., 2019; Cai et al., 2021). The reactions are accelerated in the presence of UV, therefore known as UV photo-Fenton reaction (Oturan and Aaron, 2014; Kim et al., 2019). The important radical formation steps are seen in Eqs 6, 7 while the radical termination is seen in Eqs 8, 9.

$$H_2O_2 + h\nu \rightarrow 2OH^{\cdot} \quad (6)$$

$$Fe^{3+} + H_2O + h\nu \rightarrow Fe^{2+} + OH^{\cdot} + H^+ \quad (7)$$

$$OH^{\cdot} + OH^{\cdot} \rightarrow H_2O_2 \quad (8)$$

$$Fe^{3+} + OH^{\cdot} + H^+ \rightarrow Fe^{2+} + H_2O \quad (9)$$

As part of the European Union (EU) project 'Pre-disposal management of radioactive waste' (PREDIS), technical work is being carried out internationally across EU-country labs and the United Kingdom. This focuses on innovations in nuclear waste treatments, among which the management of oxalic acid as a secondary waste form is a topic. As previously mentioned, oxalic acid as a decontaminant can be applied at high or low concentrations depending on the desired balance of reaction and corrosion rates (Zhong et al., 2021). This work, carried out at the UK's National Nuclear Laboratory (NNL) and Subatech Laboratory, IMT Atlantique in France has provided an opportunity to test destruction methods using both high and low concentrations of oxalic acid collaboratively. However, the results for the destruction at higher and lower concentrations may not be directly compared due to the differences outlined in the relevant sections. At a higher concentration of oxalic acid (520 mM), destruction using heating with nitric acid with $Mn(NO_3)_2$ and $H_2O_2$, UV light with $H_2O_2$ and Fe, and ozonation has been tested by NNL. At a low concentration of oxalic acid (10 mM), the use of $H_2O_2$ in combination with heating and application of UV light was experimented for oxalic acid destruction at Subatech Laboratory, IMT Atlantique.

# 2 Materials and methods

## 2.1 Destruction of oxalic acid at higher concentration

Oxalic acid is being considered for use by Sellafield Ltd. due to its ability to capture and solubilize radionuclides. However, it is considered necessary to establish an effective method for the destruction of oxalic acid as a precaution for its release into waste streams which cannot accommodate it; evaporation methods or *in situ* intervention have both appeared to be attractive destruction methods due to the minimal intervention with existing plant infrastructure which would be required. Hence, for the destruction of oxalic acid at higher concentration starting at 520 mM, methods of heating with nitric acid and use of UV light, Fe (II) and $H_2O_2$ were experimented. A higher concentration of 520 mM oxalic acid was selected for these experiments, influenced by an existing thermal evaporator at the Sellafield nuclear site where it is thought this destruction process could be carried out, and the solubility limit of oxalic acid in high molarity nitric acid. Experiments were generally run up to a 14-day point, or until analysis indicated that the oxalic acid had been fully destroyed to the limit of detection (3 mM).

Oxalic acid dihydrate ($C_2H_2O_4{\cdot}2H_2O$), standard grade nitric acid ($HNO_3$, 70% w/w), standard grade sulfuric acid ($H_2SO_4$, 95%–98% w/w), Mohr salt ($(NH_4)_2Fe(SO_4)_2.(H_2O)_6$), hydrogen peroxide ($H_2O_2$, 30% w/v), chromium nitrate ($Cr(NO_3)_3$), nickel nitrate ($Ni(NO_3)_2$), iron (II) nitrate ($Fe(NO_3)_2$), manganese nitrate ($Mn(NO_3)_2$), potassium permanganate ($KMnO_4$), sodium hyposulfite ($Na_2S_2O_3$), amido sulfuric acid ($H_3NSO_3$), potassium iodide (KI) and ammonium molybdate ($(NH_4)_6Mo_7O_{24}$) were sourced from Fisher Scientific UK Ltd. to their highest available purity and used. 18 MΩ cm deionized water used was sourced from the laboratory water purifier system.

### 2.1.1 Heating with nitric acid

For this technique 250 mL of liquor was heated to either 50°C, 75°C or 100°C in a round bottomed flask placed within a thermostatically controlled isomantle accurate to ±3°C. To prevent the evaporation of liquor from each heated round bottomed flask, glass condensers cooled with water at approximately 10°C were employed. Each round bottom flask was equipped with three ports; one of which was used for the condenser, one for the thermostatic temperature probe, and another which was stoppered but used for taking samples of ~2 mL using a Pasteur pipette. Aliquots (1 mL) of this sample were then used for analysis once the solution had cooled to room temperature to ensure accurate volumes were analyzed.

The liquor of all experiments contained 520 mM oxalic acid and 8 M $HNO_3$. Varying concentrations of $Mn(NO_3)_2$ between 0.025 and 50 mM were also added to the experiments for catalytic purposes. A small number of experiments were also supplemented with minor concentrations of nitrates of Fe, Cr and Ni (100, 25 and 14 ppm, respectively) so as to account for the corrosion products of stainless-steel evaporator systems on the Sellafield site. For solutions also containing $H_2O_2$, the required amount of 30% w/v $H_2O_2$ was added. All solutions were made to 250 mL with the addition of 18 MΩ cm deionized water.

### 2.1.2 Use of UV light, Fe and $H_2O_2$

For this method, 250 mL solution with a starting concentration of 520 mM oxalic acid was used. Fe (II) in the form of Mohr salt (ammonium iron (II) sulfate) was also added to some experimental solutions, equating to a concentration of 5.2 mM Fe. With the solution in a clear glass Drechsel vessel, UV light at a wavelength of 365 nm was shone towards the solution; the intensity of the UV light was controlled by using either one or two UVP UVGL-58 handheld lamps. In order to initiate a photo-Fenton-like reaction, each experiment was also dosed at regular intervals with 30% w/v $H_2O_2$ to give an addition of 12 mmoles or 23 mmoles to the solution. Control experiments for this technique were also carried out without exposure of the solution to UV light. For one type of control, the glass Drechsel vessel containing an experimental solution was not exposed to the UV lamp but was left uncovered in the laboratory, therefore being exposed to environmental light. For the other control, the glass Drechsel vessel containing an experimental solution was covered entirely with aluminum foil, thereby preventing the solution from being exposed to any light. In order to direct any gases produced during the destruction process away from the operator, all vessels were fitted with an air condenser (not temperature controlled) in the port of the Drechsel vessel.

For the consistent dosing of the experiments and the regular taking of samples for analysis, the condenser was removed from the Drechsel port. When taking samples, a 1 mL volume was taken from the vessel and used for analysis. The UV lamps, if used, were turned off during dosing or sampling to avoid UV exposure to the operator.

### 2.1.3 Sampling and analysis

Samples were taken from experiments at regular intervals, each laboratory working day. Oxalic acid concentration was quantified for each sample by two analysis methods: ultraviolet-visible (UV-Vis) spectroscopy and titration with $KMnO_4$. These techniques were selected to allow for simple and quick quantification of oxalic acid

while the experiments were ongoing. For both analysis techniques, the 1 mL sample taken from the experiment was first diluted by a dilution factor (DF) of 10.

#### 2.1.3.1 UV-vis analysis

For UV-Vis analysis, 0.25 mL of the DF 10 sample was added to 10 mL of a solution containing 3 M $HNO_3$ and 0.03 M $H_3NSO_3$. Then 0.1 mL of 0.1 M $KMnO_4$ was added, and the mixture agitated by swirling the container; this was then left undisturbed for 5 min to allow a pink color to develop. After this point, two Fisherbrand™ disposable semi-micro cell cuvettes were filled with approximately 1.5 mL of the solution. The cuvettes were then each placed in a Thermo Scientific™ GENESYS™ 40 UV-Vis spectrophotometer and the solutions analyzed at 526 nm. The absorbance of the sample at this wavelength was recorded. As analysis at this wavelength produced similar results to analysis with $KMnO_4$ titration, it is not believed that interferences occurred at this wavelength.

A calibration curve using solutions of known concentrations of oxalic acid (0–0.7 M) was plotted to establish the relationship between absorbance and oxalic acid concentration. The straight-line equation from this calibration was used to calculate the concentrations of the samples taken from the experiments.

#### 2.1.3.2 $KMnO_4$ titration for oxalic acid

For the analysis by $KMnO_4$ titration, 7 mL 18 MΩ cm deionized water and 5 mL 1 M $H_2SO_4$ were added to a conical flask and agitated on a magnetic stirrer heater plate. A 3 mL aliquot of the DF 10 experimental sample was then also added to the flask, and the mixture was heated to 60°C whilst being stirred at 60 rpm. A 0.005 M $KMnO_4$ solution was prepared and added to a burette over the heated solution; this was added to the solution dropwise until a color change from colorless to pale pink. The concentration of oxalic acid in the sample was calculated by using the volume of $KMnO_4$ titrated, taking into account the DF and the molar ratio between the oxalic acid and $KMnO_4$ in the reaction shown by Eq. 10.

$$2KMnO_4 + 3H_2SO_4 + 5(COOH)_2 \rightarrow K_2SO_4 + 2MnSO_4 + 8H_2O + 10CO_2 \quad (10)$$

The limit of detection for this method was established to be 3 mM oxalic acid.

#### 2.1.3.3 Titration with $Na_2S_2O_3$

For experiments where $H_2O_2$ was added, a further analysis method was also necessary to first quantity the concentration of $H_2O_2$ in the sample. This was essential as $H_2O_2$ can react with $KMnO_4$ (Bailey and Taylor, 1937; Li et al., 2011; Sun et al., 2019; Khan, 2021), meaning that its presence interferes with the analysis outlined above and result in an overestimation of the concentration of oxalic acid in a sample.

For this analysis, the DF 10 experimental sample was added to a conical flask along with 50 mL 18 MΩ cm deionized water, 10 mL 1 M $H_2SO_4$, 12.5 mL 0.09 M KI solution and 2 drops of ammonium molybdate solution. The mixture was stirred at ambient temperature at 60 rpm. $Na_2S_2O_3$ at 0.001 M was then added dropwise from a burette until a subtle color change from colorless to pale yellow was observed. At this point, 2 mL of starch solution was then added to the flask to initiate a color change from pale yellow to black to indicate the presence of iodine. At this point, further additions of $Na_2S_2O_3$ were made from the burette until a color change from black to colorless, indicating the end point of the titration, was observed. The total volume of $Na_2S_2O_3$ titrated was then used to calculate the concentration of $H_2O_2$ in the sample, taking into account the DF and the molar ratio between the $H_2O_2$ and $Na_2S_2O_3$ in Equations 11, 12.

$$H_2O_2 + 2KI + H_2SO_4 \rightarrow I_2 + K_2SO_4 + 2H_2O \quad (11)$$

$$I_2 + 2Na_2S_2O_3 \rightarrow Na_2S_4O_6 + 2NaI \quad (12)$$

This analysis technique was used alongside the methods for oxalic acid quantification. Therefore, the calculated concentration of $H_2O_2$ from this analysis technique was subtracted from the calculated oxalic acid values. This achieved an oxalic acid quantification representative of the sample, as the interference of $H_2O_2$ with $KMnO_4$ was considered.

## 2.2 Destruction of oxalic acid at lower concentrations

The lower concentration of oxalic acid comes from the Chemical Oxidation Reduction Decontamination (CORD) process used for decontamination of stainless steels and Ni based alloys. CORD is a decontamination technique used during maintenance and decommissioning of nuclear power plants, mainly for the primary circuit and steam generator circuit (Ocken, 1999). It is a multi-step process where potassium permanganate/permanganic acid is used in the oxidation step as seen in Eq. 13, followed by oxalic acid in the destruction and reduction step, which destroys the $MnO_2$ formed during the oxidation step, and also dissolves and complexes the iron oxides, as in Eqs 14, 15 respectively (Ocken, 1999; Rivonkar et al., 2022).

$$Cr_2O_3 + 2MnO_4^- + H_2O \rightarrow 2HCrO_4^- + 2MnO_2 \quad (13)$$

$$MnO_2 + H_2C_2O_4 + 2H^+ \rightarrow Mn^{2+} + 2CO_2 + 2H_2O \quad (14)$$

$$Fe_3O_4 + 4H_2C_2O_4 \rightarrow 3FeC_2O_4 + 2H_2O + 2CO_2 \quad (15)$$

The final solution is therefore rich in oxalic acid and its destruction is a precursor to the treatment of CORD effluents, as it is seen to affect the efficiency of precipitation of chrome (Remoundaki et al., 2007; Rivonkar et al., 2022).

### 2.2.1 Oxidation by $H_2O_2$ under effects of temperature and UV

The concentration of oxalic acid was determined from the concentrations used during the CORD process (ranging from 5 mM to 18 mM) (Ocken, 1999; Rivonkar et al., 2022). A middle ground concentration of 10 mM oxalic acid (dihydrate, ACS reagent, ≥95.0%, Alfa Aesar) was used and a volume of 100 mL was used. The hydrogen peroxide (30% in water, ThermoFisher) was mixed into the solution once the solution was at the desired temperature, i.e., when the solution reached 80°C, by heating on a heating plate, in the case of high temperature tests. The parameters temperature, concentration of $H_2O_2$ and UV radiation were evaluated. The concentrations of hydrogen peroxide tested were 100 mM, 500 mM and 1 M. Tests were carried out at 80°C corresponding to the operational temperature of the CORD process. The effects of UV radiation

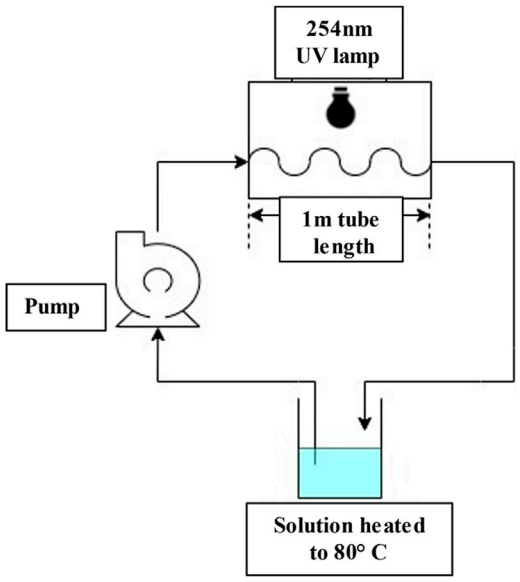


FIGURE 1
Illustration of the dynamic system used with the UV lamp.

were tested at room temperature (22°C) and at 80°C temperature, using an UV lamp (VL-6. C, 254 nm, 6W, Fisher Bioblock Scientific). The summarized methodology of the different conditions is shown in Figure 2. Contact times of 2, 4, 6 and 24 h were applied under all conditions. The measurement of oxalate concentration was carried out by taking 5 mL aliquots at all contact times and done by ion chromatography (881 Compact Pro - Anion, Metrohm) with an anion column (Metrosep A Supp 16–250/2.0, Metrohm), a flow rate of 0.15 mL/min, and a conductivity detector. The eluent used are prepared for 7.5 M $Na_2CO_3$ (anhydrous, 99.95%, Acros Organics) and 0.5 M NaOH (50%, Merck).

For the high temperature experiments using UV, the sample volume was increased to 300 mL to account for the increased volume of the loop, was placed in a glass bottle and heated on a heating plate up to 80°C and pumped through a UV chamber using a peristaltic pump (Masterflex ISM945D, 4 channels, Ismatec), at a flow rate of 10 mL/min through a Tygon R3607 flexible tube (ID 2.79 mm, Saint-Gobain Tygon LMT-55). A total length of 1 m of tube was exposed to UV which implied a contact time of 38 s. The solution was then mixed into the same bottle on the heating plate. An illustration of this setup can be seen in Figure 1. For room temperature, the solution was placed into 40 mL polypropylene bottles and placed under the UV lamp.

### 2.2.2 Influence of Mn and Fe ions

To test the influence of manganese and iron cations on the kinetics of oxalic acid destruction, three different solutions were created using salts of manganese (II) chloride (dihydrate, 99%, Merck) and iron (II) chloride (tetrahydrate, 99%, Sigma Aldrich). Concentrations of 0.8, 3 and 7.5 mM $Mn^{2+}$ and 0.14, 0.5 and 1.25 mM $Fe^{2+}$ were used, respectively. A ratio of 6:1 between Mn: Fe was maintained. The reasoning behind these values is explained in Section 3.2.3.

A summary of all the different conditions can be seen in Figure 2.

## 3 Results

### 3.1 Destruction of oxalic acid at higher concentration

#### 3.1.1 Heating in nitric acid and Mn

Figure 3 shows the data plotted from the 50°C experiments, with and without the presence of $Mn(NO_3)_2$ as a catalyst. When no manganese was present, very little oxalic acid was destroyed, and after approximately 16 days, the oxalic acid concentration was similar to the starting concentration. As the concentration of manganese increased, so did the rate of oxalic acid destruction. Very little destruction of oxalic acid was also observed at a manganese nitrate concentration of 5 mM, however at 10 mM and above, the rate of destruction increased greatly. At concentrations of 10 and 25 mM of manganese the reaction between the nitric acid and oxalic acid did not start immediately. Complete oxalic acid destruction occurred in approximately 8 days in 50 mM Mn at 50°C.

As illustrated in Figure 4, the time to completely destroy roughly 520 mM of oxalic acid can be further decreased by increasing the temperature from 50°C to 75°C. Different concentrations of manganese were added, from 0.025 to 50 mM to establish at what point the catalytic effect of the Mn at the concentration used would achieve total destruction of the oxalic acid at 75°C. Total destruction could likely be achieved without the presence of Mn, but over a considerably longer timescale than if the catalyst was used. Experiments at the highest Mn concentration (50 M and 25 mM) showed that destruction could be achieved in under 2 days.

Figure 5 shows the rate of oxalic acid destruction when heated with nitric acid at 100°C. Significantly faster oxalic acid destruction was observed with 50 mM Mn, complete destruction occurring in approximately 4 h. This time period was much longer (~30 h) when the Mn catalyst was not present under similar conditions.

Using the experimental data, the half-life (T ½) of oxalic acid under the conditions tested has been calculated, shown in Table 1. In Table 1, the time to destroy 520 mM of oxalic acid to the limit of detection under the conditions is also shown. For experiments using nitric acid only and nitric acid with 50 mM Mn, the activation energy for the destruction reaction has also been calculated. Calculation of activation energy was not possible for other experiments due to these not being carried out at all three temperatures (50°C, 75°C and 100°C). Table 1 corresponds with the trends shown in Figure 3, Figure 4 and Figure 5, with increased temperature and Mn catalyst concentration being associated with quicker oxalic acid destruction.

#### 3.1.2 Treatment via UV light, $H_2O_2$ and the addition of Fe

Figure 6 shows the results obtained from the tests focused on the destruction of oxalic acid using the photo-Fenton reaction at ambient temperature. Data showed the most effective tested conditions were using UV light, doping with 23 mmoles of $H_2O_2$

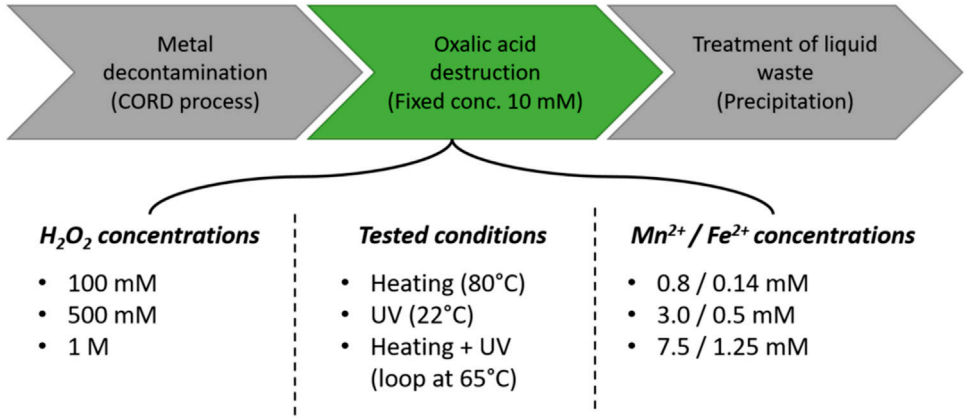


FIGURE 2
Overview of the different parameters tested in order to optimize the low concentration of oxalic acid destruction stage.

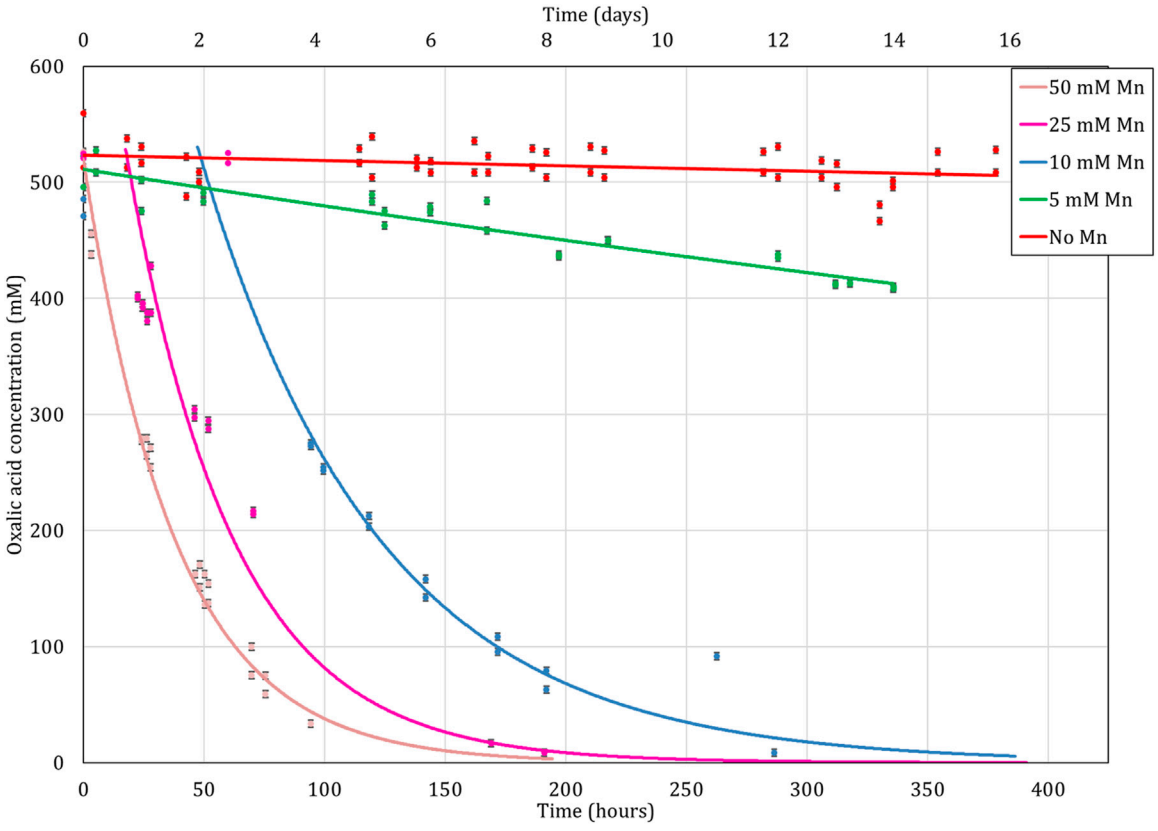


FIGURE 3
Destruction of 520 mM oxalic acid by heating with 8 M nitric acid at 50°C as a function of time. Exponential trendlines fitted.

twice each working day and the solution containing 5.2 mmoles Fe. Complete oxalic acid destruction was achieved within 6 days. When the mmoles of $H_2O_2$ was approximately halved the destruction time was extended to ~8 days. Note: a plateau in the destruction rate was observed between 2 and 4 days, which coincided with a gap in the $H_2O_2$ doping over a weekend where addition of the $H_2O_2$ was not able to be done by an operator. This plateau was not observed when the experiment was doped with 23 mmoles of $H_2O_2$ as in this case an excess of $H_2O_2$ was added, meaning there was enough $H_2O_2$ to sustain the destruction over the weekend. Additional experiments were performed to assess the impact of removing Fe and UV light. Much slower destruction was observed under these conditions, the complete destruction is estimated to be achieved in between 9 and 11 days when the data is linearly extrapolated.

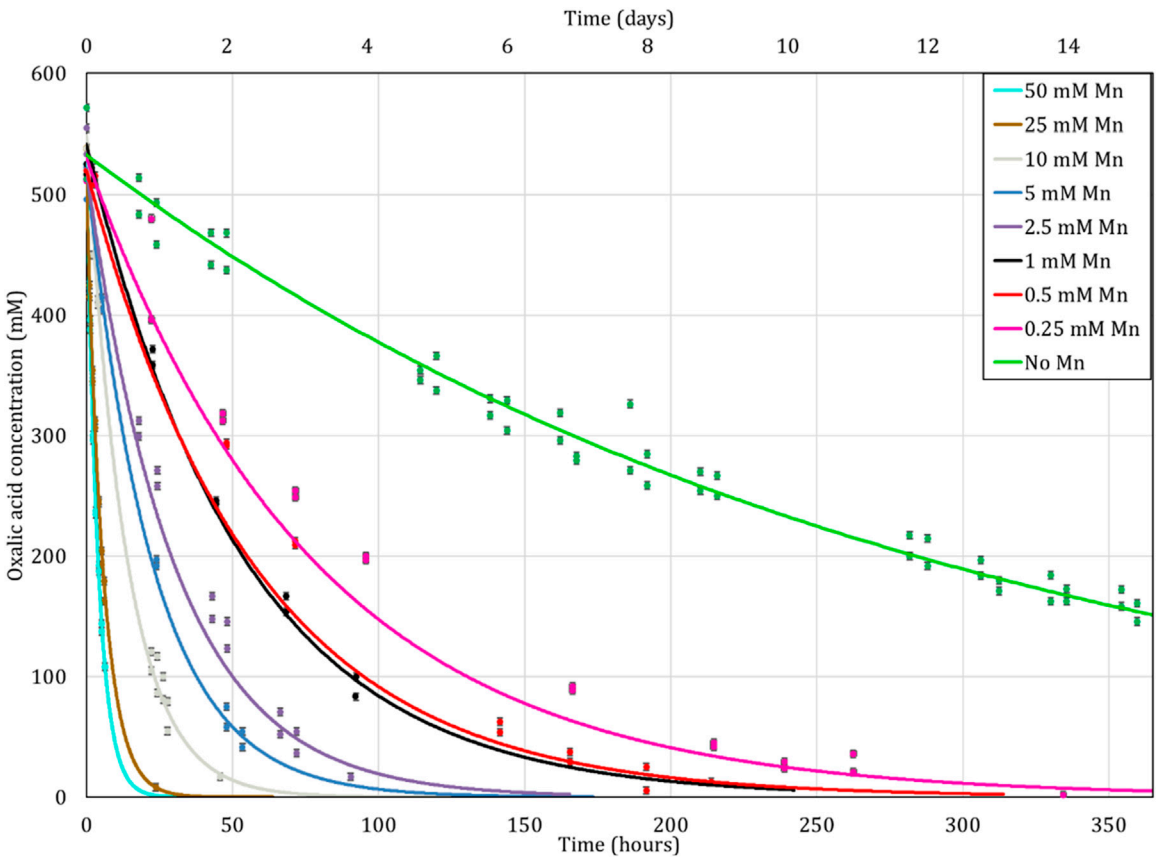


FIGURE 4
Destruction of oxalic acid by heating with 8 M nitric acid at 75°C as a function of time. Exponential trendlines fitted.

## 3.2 Destruction of oxalic acid at lower concentration

### 3.2.1 Effects of different concentrations of hydrogen peroxide

Figure 7 shows the effects of different concentrations of hydrogen peroxide observed over 24 h at 80°C, for a fixed concentration of 10 mM oxalic acid. It was observed that the efficiency of oxalic acid destruction increased as the concentration of hydrogen peroxide was increased, with the highest efficiency seen at 1 M $H_2O_2$, a ratio of 1:100 oxalic acid: hydrogen peroxide (O:H). With this ratio of 1:100, about 94% of the oxalic acid was destroyed in 24 h. It was also observed that the degradation of the oxalic acid is rapid after mixing with hydrogen peroxide and slows down as $H_2O_2$ starts to be consumed. Due to the excess of hydrogen peroxide, the rate of reaction is initially high but slows down as it is consumed. It could potentially lead to increased gas production or heat generation (exothermic reaction). As there was no sampling carried out between 6 and 24 h, the rate of degradation during this period is not precisely determined. Therefore, it is possible that the degradation stopped before 24 h.

These results were in accordance with the work published by Mailen et al. and Kim et al., who found the oxalic destruction rate increases with increasing concentration of hydrogen peroxide (Mailen et al., 1981; Kim et al., 2019). Kim et al. noticed a significant reduction in oxalic acid concentrations with a ratio of 1:2 in oxalic acid:hydrogen peroxide (O:H), albeit with the use of UV. The minimum ratio in our case was 1:10 (O:H), and the rate of destruction increased at 1:50 and was the highest at 1:100. The best-case ratio of 1:100 (O:H) was therefore selected for further tests going forward.

### 3.2.2 Effect of different conditions of treatment

Figure 8 shows the influence of UV at room temperature (22°C) and at 80°C using the system in Figure 1, in comparison to only heating at 80°C without UV exposure. At a 1:100 (O:H) ratio, it was observed that heating the solution to 80°C led to the highest degradation of oxalic acid (94% destroyed in 24 h), as in section 3.2.1, whilst exposure to UV at room temperature appeared to be least efficient (29% destroyed in 24 h). This suggests the relative inefficiency of the 6 W, 254 nm UV at the testing conditions. The combination of heating and UV lead to lower destruction efficiency as compared to just heating over 24 h, which was contradictory to section 3.2.1 and not seen in literature either. But after several tests, it was observed that the temperature of the solution at the exit of the UV chamber seen in Figure 1, was roughly 65°C, which was significantly lower than the intended temperature (80°C) used in the heating tests in the absence of UV. The loss of temperature was due to the long length of the loop, and there was no thermal insulation in place. The temperature of the bulk solution was therefore not stable at 80°C and the lower temperature would explain the lower efficiency as it led to a more gradual degradation.

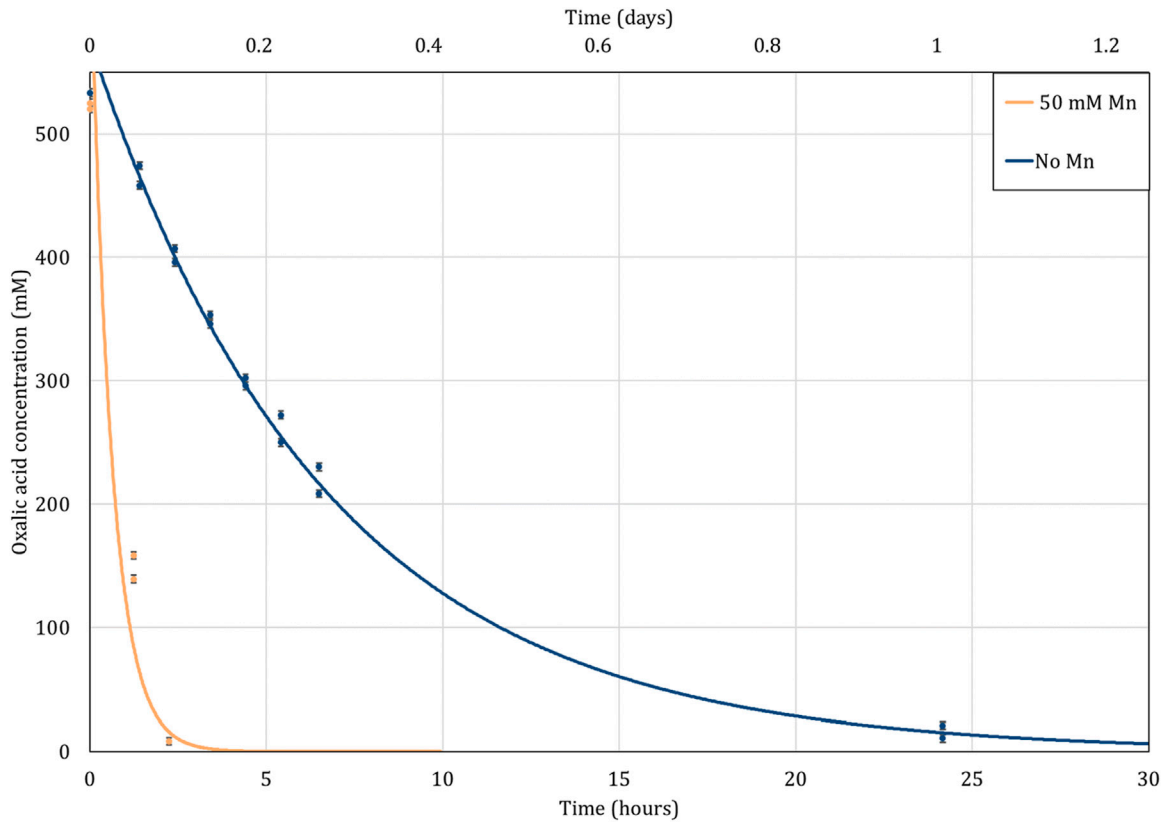


FIGURE 5
Destruction of oxalic acid by heating with 8 M nitric acid at 100°C as a function of time. Exponential trendlines fitted.

TABLE 1 Calculated half-life (hours) and calculated days taken to destroy 520 mM oxalic acid to the limit of detection under experimental conditions tested.

| | 50°C | | 75°C | | 100°C | | Activation energy (kJ $mol^{-1}$) |
|---|---|---|---|---|---|---|---|
| | *T ½ (hrs)* | *Days to destruction* | *T ½ (hrs)* | *Days to destruction* | *T ½ (hrs)* | *Days to destruction* | |
| **8 M $HNO_3$** | 10,599 | 3,401 | 205 | 66 | 5 | 2 | 154 |
| **8 M $HNO_3$ and 0.25 mM $Mn(NO_3)_2$** | - | - | 55 | 18 | - | - | - |
| **8 M $HNO_3$ and 0.5 mM $Mn(NO_3)_2$** | - | - | 40 | 13 | - | - | - |
| **8 M $HNO_3$ and 1 mM $Mn(NO_3)_2$** | - | - | 39 | 12 | - | - | - |
| **8 M $HNO_3$ and 2.5 mM $Mn(NO_3)_2$** | - | - | 21 | 7 | - | - | - |
| **8 M $HNO_3$ and 5 mM $Mn(NO_3)_2$** | 979 | 314 | 16 | 5 | - | - | - |
| **8 M $HNO_3$ and 10 mM $Mn(NO_3)_2$** | 52 | 19 | 10 | 3 | - | - | - |
| **8 M $HNO_3$ and 25 mM $Mn(NO_3)_2$** | 31 | 11 | 4 | 1 | - | - | - |
| **8 M $HNO_3$ and 50 mM $Mn(NO_3)_2$** | 27 | 9 | 3 | 0.9 | 0.5 | 0.1 | 81 |

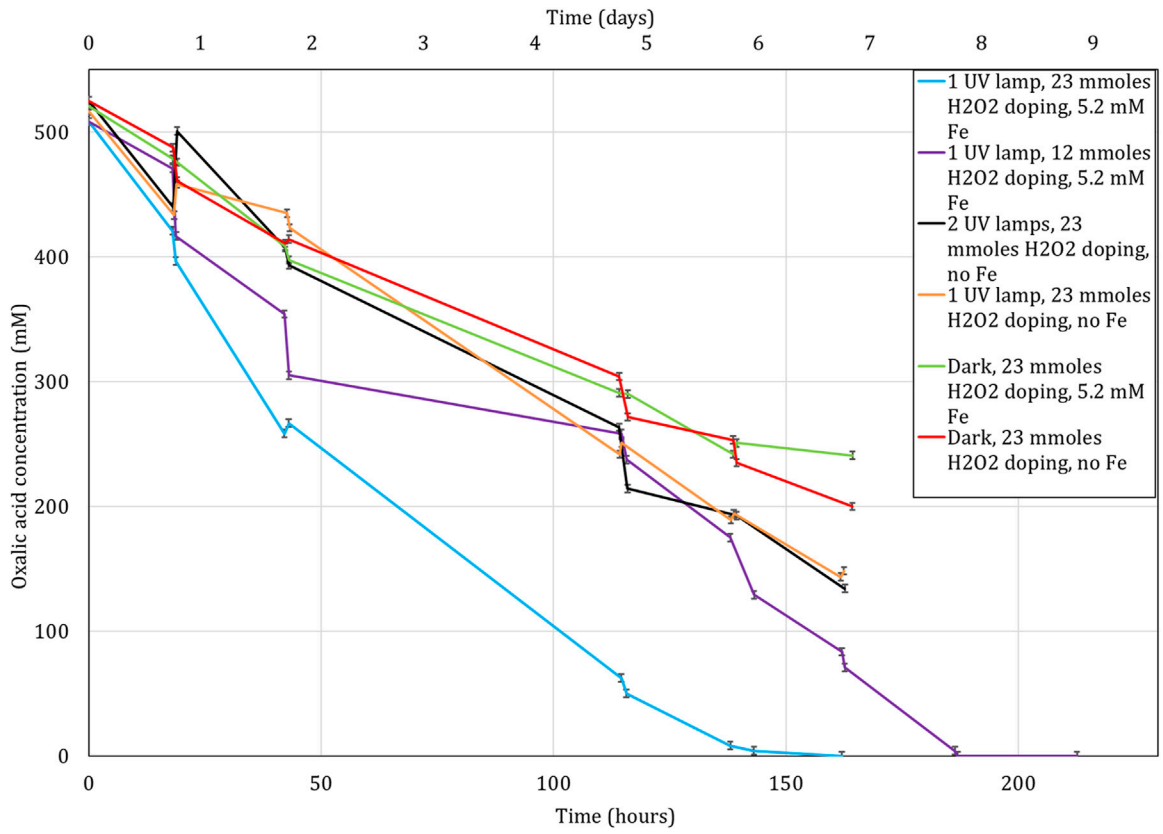


FIGURE 6
Destruction of oxalic acid by UV light, $H_2O_2$ and Fe as a function of time. $H_2O_2$ addition is given in mmoles as this is the amount added to the experiment periodically twice each working day. Lines drawn to guide the eye.

These results using the UV source are in contrast to the work done by Kim et al. and Ketusky et al., who found a 254 nm UV source to significantly affect the reaction rate and therefore the oxalic destruction rate even at lower $H_2O_2$ concentrations. A couple of hypotheses for this could be drawn with the fact that the power of the UV source in our testing was only 6 W as opposed to 120 W used during the testing by Kim et al., and 1500 W used the decomposition loop of Ketusky (2018); Ketusky et al. (2010). Further reducing the efficiency of the 6 W source used, was the fact that our tests utilized comparatively higher concentrations of $H_2O_2$ beginning from 100 mM up to 1 M, while Kim et al. described a significantly lower UV transmittance (%) even at 50 mM at 120 W (Kim et al., 2019). This would suggest the combination of higher concentration and lower power of the UV, meant an even lower transmittance through the solution.

It appears that in this scenario, the shortcomings of the UV source were overcome with the use of higher concentrations of $H_2O_2$ alongside mixing at higher temperature, which led to efficient destruction of the oxalic acid over a period of 24 h.

### 3.2.3 Effects of $Mn^{2+}$ and $Fe^{2+}$ ions on the destruction efficiency

Mn and Fe ions tend to influence the reaction by accelerating the reaction rate in the absence of UV as seen in Eqs 3–5 (Saeed et al., 2013; Kim et al., 2019; Cai et al., 2021). Their influence was studied as they are present in solution after the CORD process (Rivonkar et al., 2022). The selection of 0.8 mM $Mn^{2+}$ and 0.14 mM $Fe^{2+}$ concentrations are based on a previous work (Rivonkar et al., 2022) using the CORD process before effluent treatment. The $Mn^{2+}$ concentration is mainly coming from the $KMnO_4$ used in the CORD process whereas the $Fe^{2+}$ arises from the total dissolved iron after the CORD process. The concentrations of Mn were further increased to 3 mM and 7.5 mM, again arising from the tests done during the optimization of the CORD process published in the same work (Rivonkar et al., 2022). In the initial tests, the $Mn^{2+}$ to $Fe^{2+}$ ratio was set at 6 (with 0.8 mM $Mn^{2+}$ and 0.14 mM $Fe^{2+}$), the concentrations of $Fe^{2+}$ in the subsequent tests was increased to 0.5 mM (with 3 mM $Mn^{2+}$) and 1.25 mM (with 7.5 mM $Mn^{2+}$) in order to preserve the 6:1 ratio. This adjustment was made to simplify the testing process.

The oxalic acid destruction appears to be significantly enhanced with the presence of metallic cations as shown in Figure 9. At 1 M $H_2O_2$, at 80°C, the oxalic acid is completely decomposed after 6 h of agitation for metal concentrations of 7.5 mM of $Fe^{2+}$ and 1.25 mM of $Mn^{2+}$ whereas for concentrations ten times lower in $Fe^{2+}$ and $Mn^{2+}$ (0.8 and 0.14 mM), 97% of the oxalic acid is destroyed after 24 h of contact time. The impact of the metallic cations is even more apparent at short contact times. For an initial oxalic acid concentration of 10 mM, 6.1 mM is still present in solution for the sample containing the lowest concentrations of iron and manganese, 5.4 mM for the intermediate concentrations (3 mM of $Fe^{2+}$ and 0.5 mM $Mn^{2+}$) and only 2.8 mM for the highest

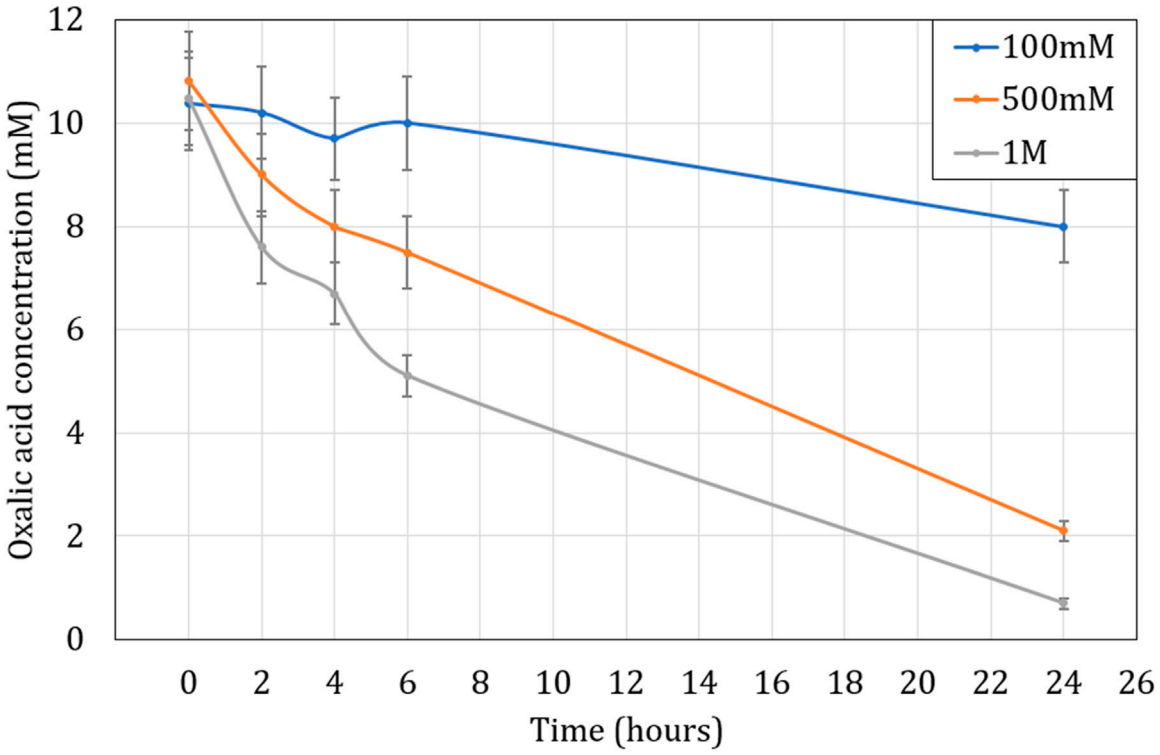


FIGURE 7
Influence of $H_2O_2$ concentration on oxalic acid concentration over time at 80°C. Initial $H_2C_2O_4$ concentration is 10 mM.

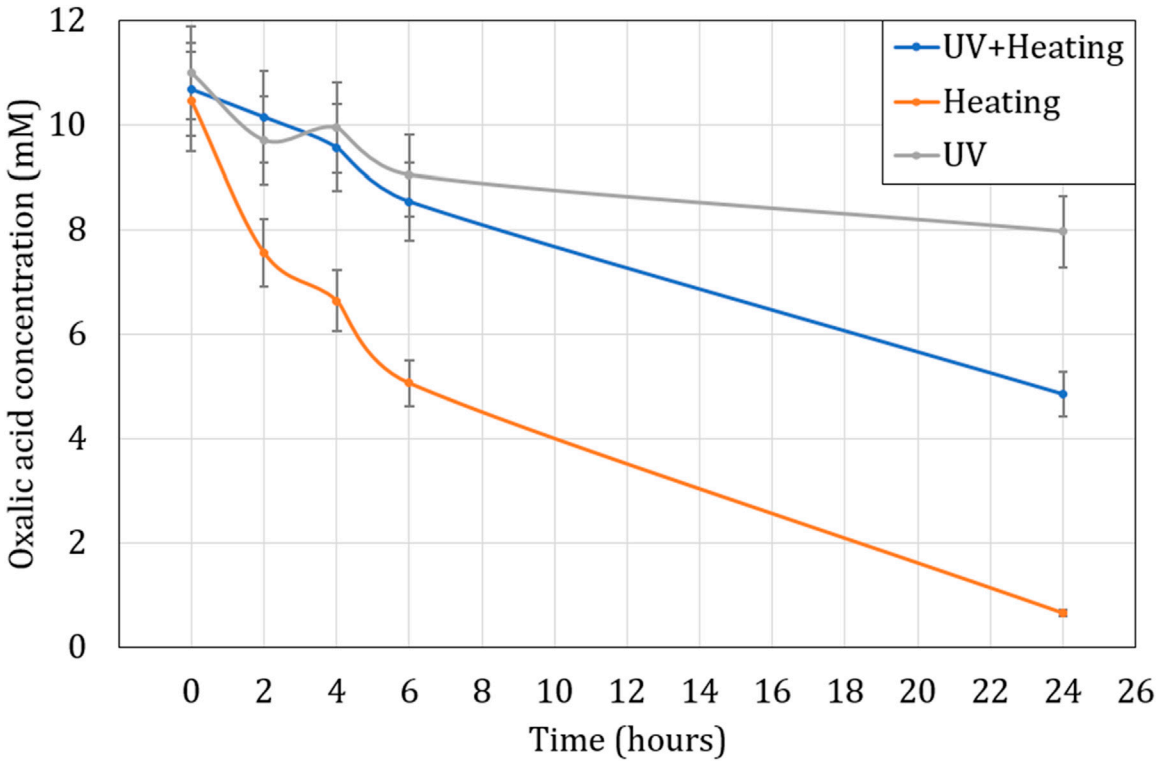


FIGURE 8
Influence of UV radiation and heating on oxalic acid oxidation over time at 80°C. Initial concentration of $H_2C_2O_4$ is 10 mM. Ratio of 1:100 (O:H).

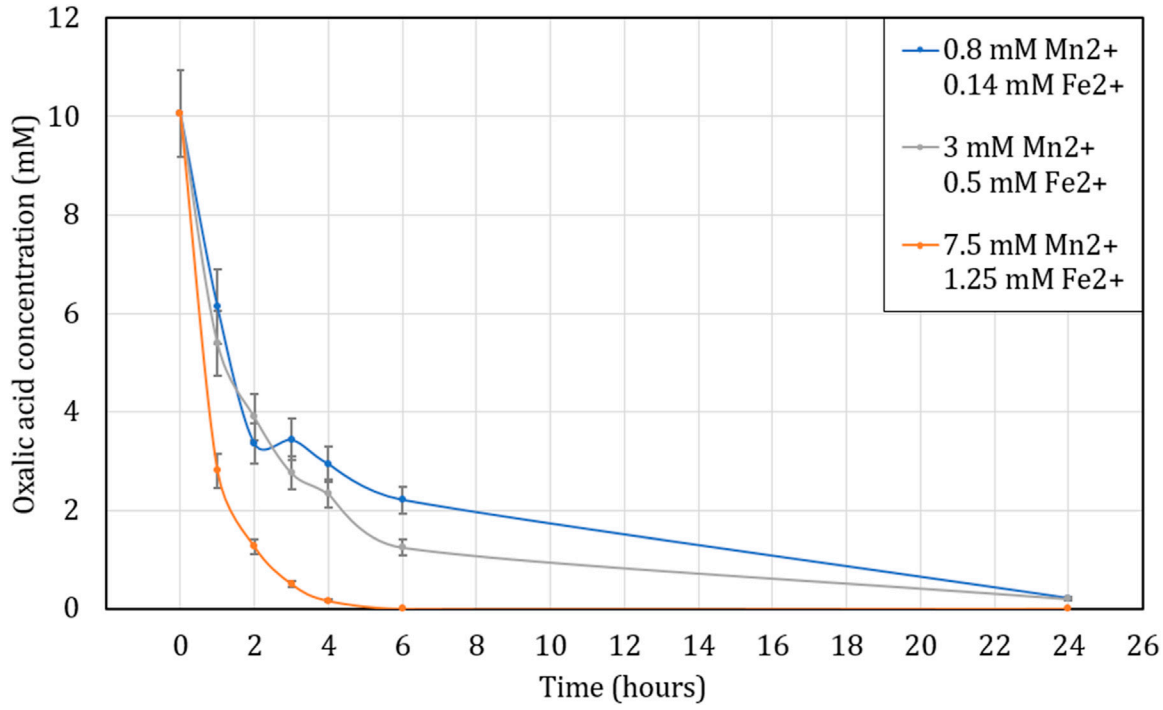


FIGURE 9
Influence of $Mn^{2+}$ and $Fe^{2+}$ concentration on oxalic acid concentration over time while heating the solution to 80°C. Initial concentration of $H_2C_2O_4$ is 10 mM. Ratio of 1:100 (O:H).

concentrations which gives a destruction 39%, 46% and 72% respectively in just 1 h.

These results are in line with the research found in literature (Kubota, 1982; Saeed et al., 2013; Kim et al., 2019; Cai et al., 2021). They found the presence of metal cations and especially $Mn^{2+}$ in solution during the destruction of oxalic acid accelerates the kinetics of this reaction. These results also show the correlation between the metal concentration and the reaction kinetics of oxalic acid destruction. The higher the metal cation concentration, the faster the decomposition of oxalic acid. Due to the presence of both Mn and Fe in CORD solutions, the effects of these ions were not studied individually, and therefore the critical ion amongst Mn and Fe, if any, cannot be identified.

### 3.2.4 Effects of UV lamp under the influence of $Mn^{2+}$ and $Fe^{2+}$ ions

The influence of metal cations in solution during the destruction of oxalic acid was also tested in a closed loop system in the presence of UV light as in Figure 1. The initial solution was heated to 80°C but the temperature decreased in the loop tube as stated previously, so an average temperature of 65°C is considered during this experiment.

The results are presented in Figure 10 and, as in the previous experiment, the presence of cations accelerates the reaction kinetics of oxalic acid destruction, although slower than in the absence of UV in section 3.2.3, possibly due to lower reaction temperature (65°C). Indeed, in the presence of a high concentration of iron and manganese (7.5 and 1.25 mM) oxalic acid decomposes by more than 70, 86% and 98% after 2, 6 and 24 h of contact respectively. For lower cation concentrations (0.8 mM $Mn^{2+}$ and 0.14 mM $Fe^{2+}$), the destruction of oxalic acid seems to be slower since its efficiency of destruction is just 32, 50% and 80% for 2, 6 and 24 h of contact time, respectively.

However, the effects of the UV lamp cannot be concretely established as described by Kim et al. (2019); Ketusky (2018); Ketusky et al. (2010). Like in Figure 7, Figure 8 does not show a benefit of using the UV but once again, this is probably due to the reasons mentioned in the previous section 3.2.2, namely, a different power for the UV lamp but also a different solution temperature due to the use of the loop.

## 4 Discussion and perspectives

This study has provided valuable insights into the crucial factors influencing the destruction of oxalic acid under various conditions and the catalytic effects of Mn coming from $Mn(NO_3)_2$ and metallic cations (Fe and Mn) coming from the decontamination of metallic wastes. The results underscore the significant impact of temperature, catalyst concentration, and UV exposure on the efficiency of oxalic acid degradation.

At higher concentrations of oxalic acid, the presence of Mn as a catalyst demonstrated remarkable potential in accelerating the rate of oxalic acid destruction, showing a positive correlation between catalyst concentration and reaction kinetics. Elevating the reaction temperature to 75°C further expedited the decomposition process, with a minimum concentration of 0.5 mM $Mn^{2+}$ required for complete destruction. Notably, higher concentrations of $Mn^{2+}$

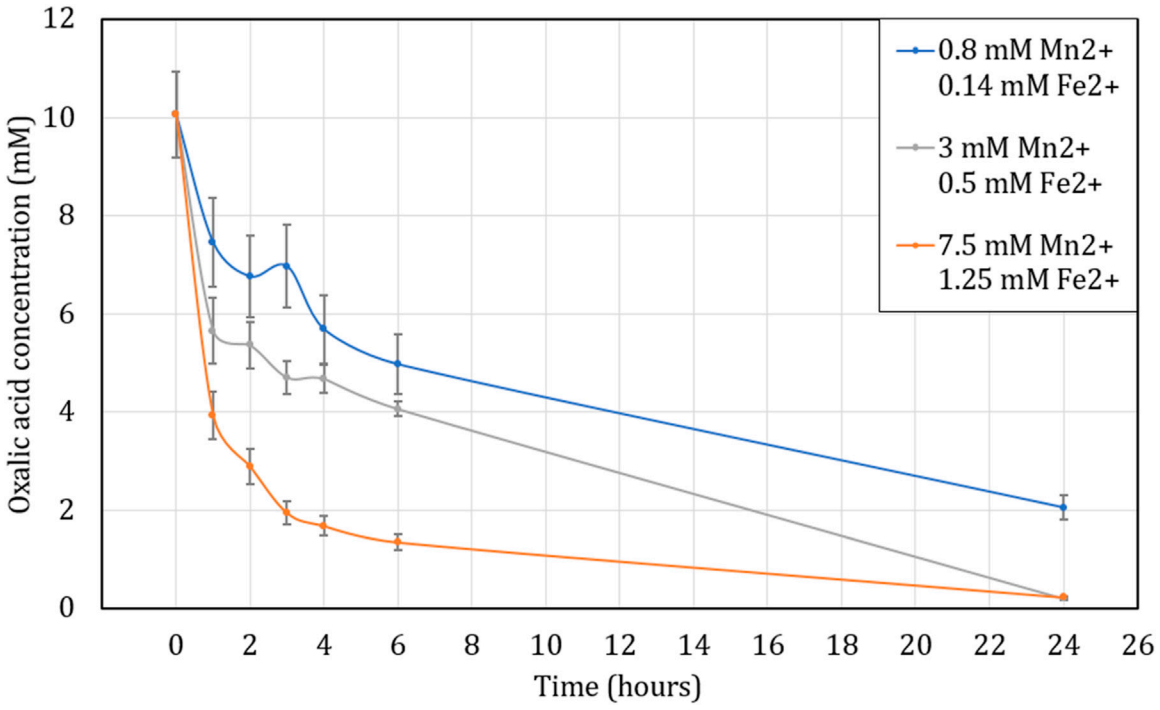


FIGURE 10
Influence of $Mn^{2+}$ and $Fe^{2+}$ concentration on oxalic acid concentration over time while heating the solution to an average of 65°C under UV lamp due to temperature loss through the loop. Initial concentration of $H_2C_2O_4$ is 10 mM. Ratio of 1:100 (O:H).

(25 mM and 50 mM) achieved rapid destruction within just 2 days. Elevating the temperature to 100°C achieved rapid destruction in less than 2 days of the oxalic acid even without presence of the catalyst.

For the photo-Fenton reaction at ambient temperature, the most effective conditions for complete oxalic acid destruction were identified, with an UV lamp, 23 mmoles $H_2O_2$ doping twice daily, and a solution containing 5.2 mM $Fe^{2+}$ exhibiting optimal results. The absence of $Fe^{2+}$ and UV light resulted in notably slower destruction rates, highlighting their crucial roles as accelerators in the process.

At lower concentrations of oxalic acid, the study investigated the effects of different $H_2O_2$ concentrations and found a 1:100 ratio of oxalic acid to hydrogen peroxide to be the most optimal for the concentrations tested. Additionally, heating to 80°C displayed high degradation efficiency, while UV exposure at various temperatures showed comparatively lower efficiency, potentially due to limitations in UV transmittance and UV source power in addition to the loss of temperature through the loop.

The presence of metallic cations ($Fe^{2+}$ and $Mn^{2+}$) significantly enhanced the destruction of oxalic acid, with higher concentrations leading to accelerated degradation rates. The study revealed a notable increase in destruction efficiency as the concentration of $Mn^{2+}$ (and therefore $Fe^{2+}$) increased, though the individual effects of $Mn^{2+}$ and $Fe^{2+}$ were not studied.

These findings hold significant implications for industrial and environmental applications, particularly in the nuclear industry where oxalic acid plays a critical role in decontamination techniques like the CORD process. Efficient and sustainable methods for destroying oxalic acid wastes are of paramount importance, and the knowledge gained from this study offers a pathway for improved degradation methods.

Future investigations could explore combining the conditions from the lower concentration oxalic acid destruction study, utilizing higher concentrations of $H_2O_2$ at 80°C in the presence of metallic cations like $Mn^{2+}$ for destruction of higher concentrations of oxalic acid. Additionally, the effects of more powerful UV sources and different wavelengths could be studied under these conditions.

Further research should also include pilot-scale experiments to validate the scalability of these results for practical applications. As the volumes of oxalic acid wastes increase, ensuring scalability is crucial for proper waste management.

Industrial stakeholders seeking effective chemical decontamination options can leverage the information gained from this research to make informed decisions and optimize their waste treatment processes.

## 5 Conclusion

The key conclusions as a result of the work carried out are.

1. The destruction of oxalic acid at high concentrations can be successfully achieved by heating with nitric acid and a Mn catalyst, and via photo-Fenton reaction.
2. At lower oxalic acid concentrations, oxalic acid destruction was successfully achieved via use of $H_2O_2$ and heating.
3. The methods tested have identified that metallic cations $Fe^{2+}$ and $Mn^{2+}$ significantly catalyze oxalic acid destruction.

4. While further research could be carried out to combine the learning from oxalic acid destruction at both high and low concentrations, the results presented in this paper indicate that the methods investigated should be considered for the treatment of secondary chemical waste during the decommissioning of nuclear facilities.

## Data availability statement

The raw data supporting the conclusion of this article will be made available by the authors, without undue reservation.

## Author contributions

JB: Data curation, Formal Analysis, Investigation, Methodology, Validation, Visualization, Writing–original draft, Writing–review and editing. AR: Methodology, Validation, Formal analysis, Investigation, Visualization, Data curation, Supervision, Writing–original draft, Writing–review and editing. MR: Data curation, Formal Analysis, Investigation, Methodology, Validation, Visualization, Writing–original draft, Writing–review and editing. TC: Conceptualization, Funding acquisition, Project administration, Supervision, Writing–review and editing. BD: Conceptualization, Funding acquisition, Project administration, Supervision, Writing–review and editing. TS-M: Methodology, Supervision, Validation, Writing–review and editing. CP: Data curation, Formal Analysis, Investigation, Methodology, Validation, Visualization, Writing–original draft. AA: Conceptualization, Funding acquisition, Project administration, Supervision, Writing–review and editing. JS: Conceptualization, Funding acquisition, Project administration, Supervision, Writing–review and editing.

## Funding

The author(s) declare that financial support was received for the research, authorship, and/or publication of this article. This work received funding support from the National Nuclear Laboratory's Science and Technology programme (Decontamination and Decommissioning Core Science), Sellafield Ltd and the 'PREDIS' Euratom research and training programme 2019-2020 under grant agreement No 945098.

## Acknowledgments

We would like to thank Nicolas Bessaguet and Valerie Bossé, from Subatech Laboratory, IMT Atlantique, for their support and training during this work.

## Conflict of interest

Author JS was employed by Sellafield Ltd.

The remaining authors declare that the research was conducted in the absence of any commercial or financial relationships that could be construed as a potential conflict of interest.

## Publisher's note



## References

Bailey, K. C., and Taylor, G. T. (1937). 209. The retardation of chemical reactions. Part VII. The reaction between potassium permanganate and hydrogen peroxide in acid solution. *J. Chem. Soc. (Resumed)* 1937, 994–999. doi:10.1039/JR9370000994

Beltrán, F. J., Rivas, F. J., and Montero-de-Espinosa., R. (2002). Catalytic ozonation of oxalic acid in an aqueous TiO2 slurry reactor. *Appl. Catal. B Environ.* 39 (3), 221–231. doi:10.1016/S0926-3373(02)00102-9

Berry, A. (1957). *Chemical reactions between hydrogen peroxide, nitric acid and oxalic acid*. United Kingdom: United Kingdom Atomic Energy Authority Industrial Group.

Cai, Q. Q., Jothinathan, L., Deng, S. H., Ong, S. L., Ng, H. Y., and Hu, J. Y. (2021). Fenton- and ozone-based AOP processes for industrial effluent treatment. *Adv. Oxid. Process. Effl. Treat. Plants* 2021, 199–254. doi:10.1016/B978-0-12-821011-6.00011-6

Chung, D.-Y., Kim, E.-H., Shin, Y.-J., Yoo, J.-H., Choi, C.-S., and Kim, J.-D. (1995). Decomposition of oxalate by hydrogen peroxide in aqueous solution. *J. Radioanalytical Nucl. Chem. Lett.* 201 (6), 495–507. doi:10.1007/BF02162727

Dükkanci, M., and Gündüz, G. (2006). Ultrasonic degradation of oxalic acid in aqueous solutions. *Ultrason. Sonochemistry* 13 (6), 517–522. doi:10.1016/j.ultsonch.2005.10.005

Gossard, A., Lilin, A., and Faure, S. (2022). Gels, coatings and foams for radioactive surface decontamination: state of the art and challenges for the nuclear industry. *Prog. Nucl. Energy* 149, 104255. doi:10.1016/j.pnucene.2022.104255

Haber, F., Weiss, J., and J Pope, W. (1934). The catalytic decomposition of hydrogen peroxide by iron salts. *Proc. R. Soc. Lond. Ser. A - Math. Phys. Sci.* 147, 332–351. doi:10.1098/rspa.1934.0221

Ketusky, E. (2018). Remediation of spent oxalic acid nuclear decontamination solutions using ozone. *Fac. Sci. Technol.*, 1462344. SRNL-L4500-2018-00011. doi:10.2172/1462344

Ketusky, E., Huff, T., and Sudduth, C. (2010). Enhanced chemical cleaning: effectiveness of the UV lamp to decompose oxalates. Available at: https://www.osti.gov/biblio/971665.

Ketusky, E., and Subramanian, K. (2012). Advanced oxidation: oxalate decomposition testing with ozone. Available at: https://www.osti.gov/biblio/1035776.

Khan, F. (2021). Reaction between hydrogen peroxide and potassium permanganate - is it useful? - bulk peroxide. Available at: https://bulkperoxide.com/reaction-between-hydrogen-peroxide-and-potassium-permanganate-is-it-useful/(Accessed October 24, 2021).

Kim, E. H., Chung, D. Y., Park, J. H., and Yoo, J. H. (2000). Dissolution of oxalate precipitate and destruction of oxalate ion by hydrogen peroxide in nitric acid solution. *J. Nucl. Sci. Technol.* 37 (7), 601–607. doi:10.1080/18811248.2000.9714936

Kim, J. H., Lee, H. K., Park, Y. J., Lee, S. B., Choi, S. J., Oh, W., et al. (2019). Studies on decomposition behavior of oxalic acid waste by UVC photo-fenton advanced oxidation process. *Nucl. Eng. Technol.* 51 (8), 1957–1963. doi:10.1016/j.net.2019.06.011

Kliegman, R., and Geme, J. S. (2019). "Defects in metabolism of amino acids: hyperoxaluria and oxalosis," in *Nelson textbook of pediatrics* (Elsevier), 695–739.

Kubota, M. (1982). Decomposition of oxalic acid with nitric acid. *J. Radioanalytical Chem.* 75 (1), 39–49. doi:10.1007/BF02519972

Lee, D.-K., and Kim, D.-S. (2000). Catalytic wet air oxidation of carboxylic acids at atmospheric pressure. *Catal. Today* 63 (2), 249–255. doi:10.1016/S0920-5861(00)00466-1

Li, Y., Zhao, Y., and Zhu, Z. (2011). Kinetic investigation of the autocatalytic reaction between potassium permanganate and hydrogen peroxide with soft-modeling methods. *Anal. Sci.* 27 (1), 37–41. doi:10.2116/analsci.27.37

Mailen, J. C., Tallent, O. K., and Arwood, P. C. (1981). *Destruction of oxalate by reaction with hydrogen peroxide*. Oak Ridge, TN (United States): Oak Ridge National Lab. doi:10.2172/6229619

Martinez-Huitle, C. A., Ferro, S., and De Battisti, A. (2004). Electrochemical incineration of oxalic acid: role of electrode material. *Electrochimica Acta* 49 (22), 4027–4034. doi:10.1016/j.electacta.2004.01.083

Martino, C., King, W., and Ketusky, E. (2012). Actual-waste tests of enhanced chemical cleaning for retrieval of SRS HLW sludge tank heels and decomposition of oxalic acid. Available at: https://www.osti.gov/biblio/1033338.

Mason, C., Brown, T. L., Buchanan, D., and Morris, D. (2008). *The destruction of oxalic acid in TPFL evaporators 1 and 2 under normal and potential abnormal conditions*. NNL (08) 9481, 2008.

Metelitsa, D. I. (1971). Mechanisms of the hydroxylation of aromatic compounds. *Russ. Chem. Rev.* 40 (7), 563–580. doi:10.1070/RC1971v040n07ABEH001939

Mitchell, T., Kumar, P., Reddy, T., Wood, K. D., Knight, J., Assimos, D. G., et al. (2019). Dietary oxalate and kidney stone formation. *Am. J. Physiology-Renal Physiology* 316 (3), F409–F413. doi:10.1152/ajprenal.00373.2018

Nash, C. (2012). *Literature review for oxalate oxidation processes and plutonium oxalate solubility*. SRNL-STI-2012-00003. Aiken, SC (United States): Savannah River Site. doi:10.2172/1034748

Ocken, H. (1999). *Decontamination handbook*. TR 112352. Palo Alto, CA: Electric Power Research Institute.

Orr, R. M., Sims, H. E., and Taylor, R. J. (2015). A review of plutonium oxalate decomposition reactions and effects of decomposition temperature on the surface area of the plutonium dioxide product. *J. Nucl. Mater.* 465, 756–773. doi:10.1016/j.jnucmat.2015.06.058

Oturan, M. A., and Aaron, J.-J. (2014). Advanced oxidation processes in water/wastewater treatment: principles and applications. A review. *Crit. Rev. Environ. Sci. Technol.* 44 (23), 2577–2641. doi:10.1080/10643389.2013.829765

Pawar, V., and Gawande, S. (2015). An overview of the Fenton process for industrial wastewater. *IOSR J. Mech. Civ. Eng.* 2015, 127–136.

Remoundaki, E., Hatzikioseyian, A., and Tsezos, M. (2007). A systematic study of chromium solubility in the presence of organic matter: consequences for the treatment of chromium-containing wastewater. *J. Chem. Technol. Biotechnol.* 82 (9), 802–808. doi:10.1002/jctb.1742

Rivonkar, A., Katona, R., Robin, M., Suzuki-Muresan, T., Abdelouas, A., Mokili, M., et al. (2022). Optimisation of the chemical oxidation reduction process (CORD) on surrogate stainless steel in regards to its efficiency and secondary wastes. *Front. Nucl. Eng.* 1. doi:10.3389/fnuen.2022.1080954

Saeed, M., Ilyas, M., Siddique, M., and Ahmad, A. (2013). Oxidative degradation of oxalic acid in aqueous medium using manganese oxide as catalyst at ambient temperature and pressure. *Arabian J. Sci. Eng.* 38 (7), 1739–1748. doi:10.1007/s13369-013-0545-x

Santos, D. F. M., Soares, O. S. G. P., Silva, A. M. T., Figueiredo, J. L., and Pereira, M. F. R. (2021). Degradation and mineralization of oxalic acid using catalytic wet oxidation over carbon coated ceramic monoliths. *J. Environ. Chem. Eng.* 9 (4), 105369. doi:10.1016/j.jece.2021.105369

Shih, Y.-J., Huang, C.-P., Chan, Y.-H., and Huang, Y.-H. (2019). Electrochemical degradation of oxalic acid over highly reactive nano-textured γ- and α-MnO2/carbon electrode fabricated by KMnO4 reduction on loofah sponge-derived active carbon. *J. Hazard. Mater.* 379, 120759. doi:10.1016/j.jhazmat.2019.120759

Solbes-García, Á., Miranda-Vidales, J. M., Nieto-Villena, A., Salvador Hernández, L., and Narváez, L. (2017). Evaluation of the oxalic and tartaric acids as an alternative to citric acid in aqueous cleaning systems for the conservation of contemporary acrylic paintings. *J. Cult. Herit.* 25, 127–134. doi:10.1016/j.culher.2016.11.013

Sun, Y., Liu, H., Tan, X., Zheng, L., Du, Y., Zheng, A., et al. (2019). Highly efficient redox reaction between potassium permanganate and 3,3′,5,5′-tetramethylbenzidine for application in hydrogen peroxide based colorimetric assays. *RSC Adv.* 9 (4), 1889–1894. doi:10.1039/C8RA07758D

Wang, F., Wu, P., Chen, M., Wu, J., Sun, L., Shang, Z., et al. (2023). Green rust sulfate transformation under the impact of Cr(VI) and oxalic acid: mechanism and environmental significance. *Appl. Clay Sci.* 233, 106825. doi:10.1016/j.clay.2023.106825

Wang, Q., Wang, F., Cai, C., Chen, H., Ji, F., Chen, Y., et al. (2023). Laser decontamination for radioactive contaminated metal surface: a review. *Nucl. Eng. Technol.* 55 (1), 12–24. doi:10.1016/j.net.2022.09.020

Zhang, G., Hu, J., and Xu, H. (2022). Oxalic acid induced defect state graphitic carbon nitride with improved photocatalytic performance. *J. Mol. Struct.* 1249, 131611. doi:10.1016/j.molstruc.2021.131611

Zhong, L., Lei, J., Deng, J., Lei, Z., Lei, L., and Xu, X. (2021). Existing and potential decontamination methods for radioactively contaminated metals-A review. *Prog. Nucl. Energy* 139, 103854. doi:10.1016/j.pnucene.2021.103854